Parametric Shape Optimization using the Support Function

Pedro R S Antunes, Beniamin Bogosel

Parametric Shape Optimization using the Support Function

Pedro R.S. Antunes*, Beniamin Bogosel†

December 7, 2019

Abstract

The optimization of functionals depending on shapes which have convexity, diameter or constant width constraints poses difficulties from a numerical point of view. We show how to use the support function in order to approximate solutions to such problems by finite dimensional optimization problems under various constraints. After constructing the numerical framework, we present some applications from the field of convex geometry. We consider the optimization of various functionals depending on the volume, perimeter and Dirichlet Laplace eigenvalues under the constraints presented earlier. In particular we confirm numerically Meissner's conjecture, regarding three dimensional bodies of constant width with minimal volume, by directly solving an optimization problem.

1 Introduction

Shape optimization problems are a particular class of optimization problems where the variable is a shape. A typical example of such a problem has the form

$$\min_{\omega \in \mathcal{A}} \mathcal{F}(\omega), \tag{1}$$

where the functional $\mathcal{F}$ is computed in terms of the shape ω and $\mathcal{A}$ is a family of sets with given properties and eventual constraints. The cost functional $\mathcal{F}$ can be related to geometric quantities, like the volume or the perimeter of the set, or we can have a more complex dependence, via a partial differential equation. Classical examples in this sense are functionals depending on the spectrum of various operators related to ω, like the Dirichlet-Laplace operator.

When dealing with constrained shape optimization problems, having volume or perimeter constraints facilitates the study of optimizers, in particular because there exist arbitrarily small inner and outer perturbations of the boundary which preserve the constraint. This is not the case when working in the class of convex sets, when bounds on the diameter are considered or when we a fixed constant width constraint is imposed. The papers [LN10],[LNP12] describe some of the theoretical challenges when working with these constraints.

Difficulties of the same nature arise when dealing with convexity, constant width and diameter constraints from a numerical point of view. Since many techniques in numerical shape optimization rely on the existence of the shape derivative, which in turn, relies on the existence of perturbations preserving the constraint, handling these constraints numerically is not straightforward. There are works in the literature which propose algorithms that can handle the convexity constraint. In [LRO05] a convex hull method is proposed in which the convex shapes are represented as intersections of half-spaces. In [MO14] the authors propose a method

*Secção de Matemática, Departmento de Ciências e Tecnologia, Universidade Aberta, Palácio Ceia, Rua da Escola Politécnica 141-147, 1269-001 Lisbon, Portugal and Grupo de Física Matemática, Faculdade de Ciências, Universidade de Lisboa, Campo Grande, Edifício C6, P-1749-016 Lisboa, Portugal, e-mail: prantunes@fc.ul.pt

†CMAP, École Polytechnique, 91120 Palaiseau, France, e-mail: beniamin.bogosel@cmap.polytechnique.fr.

of projection onto the class of convex shapes. The articles [BLRO07], [LRO07], [Oud13] show how to deal with width constraints. The paper [BW18] shows how to handle simultaneously convexity and PDE constraints. The approach proposed considers discretized domains (typically triangulations) and imposes constraints on the deformations of the domains which preserve convexity. These methods are rather complex and not straightforward to implement. The purpose of this article is to present a more direct approach, using the properties of the support function. Such a method was already proposed in [BH12] for the study of shapes of constant width, but was essentially limited to the two dimensional. In particular, the three dimensional computations presented there are in the rotationally symmetric cases, which allows the use of two dimensional techniques. Moreover, the numerical framework in [BH12] needed special tools regarding semi-definite programming algorithms and the functional to be optimized was at most linear or quadratic.

The precise definition and properties of the support function are presented Section 2. Recall just that for a convex body $K \subset \mathbb{R}^d$ the support function p is defined on the unit sphere $\mathbb{S}^{d-1}$ and for each $\theta \in \mathbb{S}^{d-1}$, $p(\theta)$ measures the distance from a fixed origin, which can be chosen inside K, to the tangent hyperplane to K orthogonal to θ in the direction given by θ. Already from the definition it can be noted that the quantity $p(\theta) + p(-\theta)$ represents the diameter or width of the body K in the direction parallel to θ. This allows to easily transform diameter or constant width constraints into functional inequality or equality constraints in terms of the support function. Convexity constraints can be expressed in similar ways, with complexity varying in terms of the dimension d. These facts are recalled in the following section.

It is possible to build finite dimensional approximations of convex bodies using a truncation of a spectral decomposition of the support function. This can be done, for example, by using Fourier series decomposition for $d = 2$ and spherical harmonic decomposition for $d \geq 3$. Using these parametrizations convexity constraints turn into linear pointwise inequalities for $d = 2$ or quadratic pointwise inequalities for $d = 3$. Moreover, the constant width constraint can be obtained by simply imposing that the coefficients of all the even functions in the basis decomposition are zero. Diameter constraints can also be translated into pointwise linear inequalities. The advantages don't stop here: in various situations, functionals like volume and perimeter have explicit formulas in terms of the coefficients in the above decompositions.

In [BH12] the authors study numerically optimization problems under constant width constraint for $d = 2$, with the aid of the support function and Fourier series decomposition. However, they work with a global parametrization of the convexity constraint, which requires the use of specific semidefinite-programming techniques and software. We choose to work in a simplified framework, inspired from [Ant16], in which the convexity constraint is imposed on a finite, sufficiently large, number of points, giving rise to a more simple constrained optimization problem that can be handled by standard optimization software.

The use of a truncated spectral decomposition is a natural choice of discretization, but in the case of the support function it is not clear whether the solutions of the finite dimensional problems obtain converge towards the solution of the original problem. These aspects are addressed in Section 3 where theoretical aspects are shown regarding the existence of solutions to the problems considered. Moreover, the convergence of the solutions of the discrete problems towards the solution of the continuous problem is investigated.

The paper is organized as follows. In Section 2 various properties of the support function parametrization in dimension two and three are recalled. In Section 3 theoretical aspects regarding the existence of solutions and the convergence of the discrete solutions are investigated. Section 4 deals with the parametric representation of shapes using the spectral decomposition of the support function. The constraints we are interested in: convexity, constant width, diameter and inclusion are discussed. Section 5 recalls the method of fundamental solutions used for solving the Dirichlet-Laplace eigenvalue problems.

Section 6 contains a wide range of applications for various problems in convex geometry. A

new confirmation of the Meissner conjecture regarding bodies of constant width with minimal volume in dimension three is provided. The two different Meissner bodies are obtained by directly minimizing the volume under constant width constraint starting from general random initializations. Further applications presented in Section 6 are the minimization of eigenvalues of the Dirichlet-Laplace operator under convexity and constant width constraints, approximation of rotors of minimal volume in dimension three, approximation of Cheeger sets and the minimization of the area under minimal width constraint.

Originality: The goal of this paper is to present a general method for performing shape optimization under various non-standard constraints: convexity, fixed width, diameter bounds by transforming them into algebraic constraints in terms of a spectral decomposition of the support function. In order to illustrate the method, various numerical results are presented, some of which are new and are listed below:

- *optimization of the Dirichlet-Laplace eigenvalues under convexity constraint*: the case $k = 2$ in dimension two was extensively studied (see for example [AH11], [Oud04]). The case of $k \geq 3$ in dimension two and the simulations in dimension three are new and are presented in Section 6.1.
- *numerical confirmation of Meissner's conjecture*: the proposed numerical framework allows to obtain Meissner's bodies when minimizing the volume under fixed width and convexity constraints, starting from randomized initial spherical harmonics coefficients. This result is presented in Section 6.2.
- *minimization of the Dirichlet-Laplace eigenvalues under volume and fixed width constraint in dimension three*: in Figure 4 some cases where the ball is not optimal are presented.
- *rotors of minimal volume in dimension three*: the numerical framework allows to find candidates for the optimal rotors in the regular tetrahedron and the regular octahedron. The results are shown in Figure 6.

Other results, which may not be new, deal with the computation of Cheeger sets for various two dimensional and three dimensional domains and the minimization of area of a three dimensional body under minimal width constraint.

2 Support function parametrization

This section recalls some of the main properties of the support function, as well as the properties which will be used in order to implement numerically the various constraints of interest in this work. The references [Sch14], [BH12], [AG11] and [ŠGJ08] contain more details about this subject.

Let B be a convex subset of $\mathbb{R}^d$. The support function of B is defined on the unit sphere $\mathbb{S}^{d-1}$ by

$$p(\theta) = \sup_{x \in B} \theta.x,$$

where the dot represents the usual Euclidean dot product. Geometrically, $p(\theta)$ represents the maximal distance from the origin to a tangent plane α to B such that α is orthogonal to θ, taking into account the orientation given by θ. Given this interpretation, it is not hard to see that the sum of the values of the support function for two antipodal points will give the *width* or diameter of B in the direction defined by these two points. This already shows that bounds on the width of B could be expressed by inequalities of the type

$$w \leq p(\theta) + p(-\theta) \leq W \text{ for every } \theta \in \mathbb{S}^{d-1} \tag{2}$$

and a constant width constraint can be expressed by

$$w = p(\theta) + p(-\theta) \text{ for every } \theta \in \mathbb{S}^{d-1}. \tag{3}$$

As already shown in [Ant16], it is possible to impose inclusion constraints when dealing with support functions. Consider two convex bodies B_1, B_2 with support functions given by p_1, p_2. Then B_1 is included in B_2 if and only if $p_1(\theta) \leq p_2(\theta)$ for every $\theta \in \mathbb{S}^{d-1}$. In the case where B_2 is an intersection of half-spaces the inequality $p_1(\theta) \leq p_2(\theta)$ needs to be imposed only for a finite number of directions $\theta \in \mathbb{S}^{d-1}$, corresponding to the normals to the hyperplanes determining the hyperspaces.

Each convex body in $\mathbb{R}^d$ has its own support function. It is not true, however, that every support function $p : \mathbb{S}^{d-1}$ generates a convex body. The necessary assumptions for a function to be the support function of a convex body are presented below.

Given a convex set B and its support function p, a parametrization of ∂B is given by

$$\mathbb{S}^{d-1} \ni u \mapsto p(u).u + \nabla_\tau p(u) \in \mathbb{R}^d,$$

where ∇_τ represents the tangential gradient with respect to the metric in $\mathbb{S}^{d-1}$. Note that for this parametrization the normal of the point corresponding to $u \in \mathbb{S}^{d-1}$ is exactly u. The convexity constraint could be expressed by the fact that the principal curvatures of the surface are everywhere non-negative. In the following, the presentation is divided with respect to the dimension.

2.1 Dimension 2

In $\mathbb{R}^2$, the unit circle $\mathbb{S}^1$ is identified to the interval $[0, 2\pi]$, therefore the parametrization of the boundary of the shape in terms of the support function becomes

$$\begin{cases} x(\theta) = p(\theta)\cos\theta - p'(\theta)\sin\theta \\ y(\theta) = p(\theta)\sin\theta + p'(\theta)\cos\theta. \end{cases} \tag{4}$$

It is immediate to see that $\|(x'(\theta), y'(\theta))\| = p(\theta) + p''(\theta)$ and, as already underlined in [BH12], the convexity constraint in terms of the support function is $p + p'' \geq 0$ in the distributional sense.

2.2 Dimension 3

In $\mathbb{R}^3$ it is classical to consider the parametrization of $\mathbb{S}^2$ given by

$$\mathbf{n} = \mathbf{n}(\phi, \psi) \mapsto (\sin\phi\sin\psi, \cos\phi\sin\psi, \cos\psi),\ \phi \in [-\pi, \pi), \psi \in (0, \pi). \tag{5}$$

As recalled in [ŠGJ08], if $p = p(\phi, \psi)$ is a C^1 support function then a parametrization of the boundary is given by

$$\mathbf{x}_p(\phi, \psi) = p(\phi, \psi)\mathbf{n} + \frac{p_\phi(\phi, \psi)}{\sin^2\psi}\mathbf{n}_\phi + p_\psi(\phi, \psi)\mathbf{n}_\psi \tag{6}$$

Moreover, it is possible to write explicitly the differential $d\mathbf{x}_p$ on the basis $\mathbf{n}_\phi, \mathbf{n}_\psi$ of the tangent space at $\mathbb{S}^2$:

$$d\mathbf{x}_p|_{\mathbf{n}}(\mathbf{n}_\phi) = \left(p\sin\psi + \frac{p_{\phi\phi}}{\sin\psi} + p_\psi\cos\psi\right)\frac{\mathbf{n}_\phi}{\sin\psi} + \left(-\frac{p_\phi\cos\psi}{\sin\psi} + p_{\psi\phi}\right)\mathbf{n}_\psi \tag{7}$$

$$d\mathbf{x}_p|_{\mathbf{n}}(\mathbf{n}_\psi) = \left(\frac{p_{\phi\psi}}{\sin\psi} - \frac{p_\phi\cos\psi}{\sin^2\psi}\right)\frac{\mathbf{n}_\phi}{\sin\psi} + (p + p_{\psi\psi})\mathbf{n}_\psi. \tag{8}$$

Note that $\{\mathbf{n}_\phi/\sin(\psi), \mathbf{n}_\psi\}$ is an orthonormal basis of the tangent space. The convexity constraint amounts to imposing that the principal curvatures are everywhere non-negative. This

is equivalent to the fact that the eigenvalues of the matrix with coefficients given by the differential of $\mathbf{x}_h$ are non-negative for every $\phi \in [-\pi, \pi)$ and $\psi \in [0, \pi)$. In dimension 3 it is enough to impose a simpler condition. Indeed, if a surface has non-negative Gaussian curvature in a neighborhood of a point, then the surface is locally convex around that point. Tietze's theorem states that if a set is locally convex around each point then it is globally convex [Val64, p. 51-53]. Moreover, a direct reference to the fact that a closed surface in dimension 3 which has positive Gaussian curvature everywhere bounds a convex body can be found in [Top06, p. 108]. This is also known as Hadamard's Problem. Therefore, in dimension three, the convexity constraint can be imposed by assuring that the Gaussian curvature is positive at every point. Therefore the determinant of the matrix containing the coefficients of the differential written above should be positive:

$$\left(p \sin\psi + \frac{p_{\phi\phi}}{\sin\psi} + p_\psi \cos\psi\right)(p + p_{\psi\psi}) + \frac{1}{\sin\psi}\left(\frac{p_\phi \cos\psi}{\sin\psi} - p_{\psi\phi}\right)^2 > 0 \tag{9}$$

for every $\phi \in [-\pi, \pi),\ \forall \psi \in (0, \pi)$.

Note that formulas (6), (7), (8) and (9) contain $\sin\psi$ in some of the denominators. In the numerical simulations the discretization of the sphere is always chosen avoiding the north and south poles of the sphere $\mathbb{S}^2$ where $\sin\psi$ cancels and where singular behavior may occur.

3 Theoretical aspects

3.1 Existence of optimal shapes

When dealing with shape optimization problems, one of the first questions posed is the existence of solutions. All problems studied numerically in this article deal with convex domains contained in a bounded set, so it is useful to define the class $\mathcal{K}^d$ of closed convex sets in $\mathbb{R}^d$ which are contained in a closed ball B. The question of existence of solutions is greatly simplified due to the following result.

Theorem 1 (Blaschke's selection theorem)**.** *Given a sequence $\{K_n\}$ of closed convex sets contained in a bounded set, there exists a subsequence which converges to a closed convex set K in the Hausdorff metric.*

For the sake of completeness, recall that the Hausdorff distance between two convex bodies K_1, K_2 is defined by

$$d_H(K_1, K_2) = \max\left\{\sup_{x\in K_1}\inf_{y\in K_2}|x-y|, \sup_{x\in K_2}\inf_{y\in K_1}|x-y|\right\}.$$

A sequence of closed convex sets $\{K_n\}$ converges to K in the Hausdorff metric if and only if $d(K, K_n) \to 0$ as $n \to \infty$.

More details regarding this result and a proof can be found in [HP18, Chapter 2]. Existence results for all problems found in the following come from the properties listed below. These properties are classical, but are recalled below from the sake of completeness, with sketches of proof when the proofs were not readily found in the literature. If K_1, K_2 have support functions p_{K_1} and p_{K_2} then the Hausdorff distance is simply $d_H(K_1, K_2) = \|p_{K_1} - p_{K_2}\|_\infty$ [Sch14, Lemma 1.8.14].

Property 1. *Convexity is preserved by the Hausdorff convergence.*

For a proof see [HP18, p. 35].

Property 2. *If $\{K_n\}$ is a sequence of non-empty closed convex sets contained in a bounded set then the Hausdorff convergence of K_n to K is equivalent to the uniform convergence of the support functions p_{K_n} to p on $\mathbb{S}^{d-1}$.*

For a proof see [SW79, Theorem 6].

In the following, χ_K denotes the characteristic function of the set K.

Property 3. *Suppose that the sequence of convex sets $\{K_n\}$ converges to the convex set K in the Hausdorff topology and that K has non-void interior. Then χ_{K_n} converges to χ_K in L^1. As a consequence, $|K_n| \to |K|$ and $\mathcal{H}^{d-1}(\partial K_n) \to \mathcal{H}^{d-1}(K)$ as $n \to \infty$.*

A proof of this fact can be found in [BB05, Proposition 2.4.3].

The Dirichlet-Laplace eigenvalues are solutions of The eigenvalue problem related to the Laplace equation has the form

$$\left\{ \begin{array}{rcll} -\Delta u & = & \lambda_k(\omega) u & \text{in } \omega \\ u & = & 0 & \text{on } \partial\omega. \end{array} \right. \tag{10}$$

It is classical that for Lipschitz domains, the spectrum of the Dirichlet-Laplace operator consists of a sequence of eigenvalues (counted with multiplicity)

$$0 < \lambda_1(\omega) \leq \lambda_2(\omega) \leq ... \to \infty.$$

In particular, convex sets with non-void interior enter into this framework.

The following property deals with the continuity of these eigenvalues with respect to the Hausdorff metric.

Property 4. *If K_n are convex and converge to K in the Hausdorff metric then K_n γ-converges to K and, in particular the eigenvalues of the Dirichlet-Laplace operator are continuous: $\lambda_k(K_n) \to \lambda_k(K)$.*

For more details see [Hen06, Theorem 2.3.17].

Property 5. *Inclusion is stable for the Hausdorff convergence: $K_n \subset \Omega$, $K_n \to K$ implies $K \subset \Omega$.*

For a proof see [HP18, p. 33].

Property 6. *The diameter and width constraints are continuous with respect to the Hausdorff convergence of closed convex sets. In particular if the sequence of closed convex sets $\{K_n\}$ converges to K in the Hausdorff metric and each K_n is of constant width w then K is also of constant width w.*

Proof: Property 2 recalled above shows that the Hausdorff convergence implies the uniform convergence of support functions on $\mathbb{S}^{d-1}$. Therefore, diameter and width constraints that can be expressed in pointwise form starting from the support functions are preserved, in particular, the constant width property. □

In the following, $\{\phi_i\}_{i=1}^{\infty}$ denotes a basis of $L^2(\mathbb{S}^{d-1})$ made of eigenvalues of the Laplace-Beltrami operator on $\mathbb{S}^{d-1}$ (the Fourier basis in 2D and the spherical harmonics in 3D). Denote by $\lambda_i \geq 0$, $i \geq 0$, the corresponding eigenvalues: $-\Delta_\tau \phi_i = \lambda_i \phi_i$ on $\mathbb{S}^{d-1}$. When studying rotors, only some of the coefficients in the spectral decomposition are non-zero. Also, in numerical approximations a truncation of the spectral decomposition is used. Therefore, it is important to see if such a property is preserved by the Hausdorff convergence of convex sets. Let $J \subset \mathbb{N}$ be a non-empty, possibly infinite subset and denote by

$$\mathcal{F}_J = \{p : p = \sum_{i=0}^{\infty} \alpha_i \phi_i, p \text{ is the support function of a convex body}, \alpha_i = 0 \ \ \forall i \notin J\},$$

i.e. convex shapes for which the coefficients with indices that are not in the set J are zero. The following result holds:

Property 7. *For a fixed set $J \subset \mathbb{N}$, let $\{K_n\}$ be a sequence of closed convex sets contained in a bounded set B with support functions (p_{K_n}) contained in $\mathcal{F}_J$ such that K_n converge to K in the Hausdorff topology. Then the support function of K also belongs to $\mathcal{F}_J$.*

Proof: From Property 2 it follows that the support functions of K_n converge uniformly to the support function of K, i.e. $\|p_{K_n} - p_K\|_\infty \to 0$ as $n \to \infty$. This obviously implies the convergence in L^2 of the support functions. In particular, if $p_K = \sum_{i=1}^{\infty} \alpha_i \phi_i$ and $p_{K_n} = \sum_{i=1}^{\infty} \alpha_i^n \phi_i$ then

$$\int_{\mathbb{S}^{d-1}} (p_{K_n} - p_K)\phi_i = \alpha_i^n - \alpha_i.$$

Since the left hand side converges to zero as $n \to \infty$ for all i, it follows that $\alpha_i^n \to \alpha_i$ for all i. In particular, if $i \notin J$ then all $\alpha_i^n = 0$. As a consequence $\alpha_i = 0$ for all $i \notin J$, which means that $p_K \in \mathcal{F}_J$. □

As underlined in Section 2 it is possible to characterize constant width bodies by imposing that certain coefficients of the support function are zero. Therefore, property 7 also implies that if a sequence of closed convex bodies of constant width K_n converges in the Hausdorff metric to K then K is also of constant width, as recalled in Property 6.

It is possible now to prove the existence of solutions for all problems studied numerically in the following section. Recall that $\lambda_k(\Omega)$ denotes the k-th eigenvalue of the Dirichlet-Laplace operator defined by (10).

Problem 1 (**Minimizing Dirichlet-Laplace eigenvalues under convexity constraint.).**

$$\min\{\lambda_k(\Omega) : \Omega \subset \mathbb{R}^N, \Omega \textit{ convex }, |\Omega| = c.\}$$

The existence of solutions for this problem is proved in [Hen06, Theorem 2.4.1]. It is a direct consequence of Theorem 1 and Properties 3, 4 above.

Problem 2 (**Minimize the eigenvalues** (10) **under convexity and constant-width constraints.).**

$$\min\{\lambda_k(\Omega) : \Omega \subset \mathbb{R}^N, \Omega \textit{ convex with fixed constant width }, |\Omega| = c.\}$$

For proving the existence in this case, choose a minimizing sequence $\{K_n\}$ which, by Theorem 1, up to a subsequence, converges to K. In view of the Properties 3, 4 and 6 above K is indeed a solution.

Problem 3 (**Minimizing the volume under constant width constraint.).**

$$\min\{|\Omega| : \Omega \subset \mathbb{R}^N, \Omega \textit{ convex with fixed constant width }\}$$

The existence follows from Properties 3, 6 when working with a converging minimizing sequence, which exists by Theorem 1.

The next problem considered concerns rotors of minimal volume. A rotor is a convex shape that can be rotated inside a polygon (or polyhedron) while always touching every side (or face). A survey on rotors in dimension two and three can be found in [Gol60]. In particular, the article [Gol60] describes which coefficients are non-zero in the spectral decomposition of the support function of rotors, using Fourier series in 2D or spherical harmonics in 3D. It turns out that the earliest complete development on the subject was published in 1909 by Meissner [Mei09]. More details and proofs of the claims in the papers described above can be found in [Gro96].

In dimension two, every regular n-gon admits non-circular rotors and they are characterized by the fact that only the coefficients for which the index has the form $nq \pm 1$ are non-zero, where q is a positive integer. In dimension three, there are only three regular polyhedra which admit rotors: the regular tetrahedron, the cube and the regular octahedron. The rotors in a cube are bodies of constant width. For rotors in a tetrahedron the only non-zero coefficients correspond to the spherical harmonics of index $0, 1, 2$ and 5, while in the case of the octahedron the non-zero coefficients are of index $0, 1$ and 5. The constant term in the spectral decomposition of the support function of a rotor corresponds to the inradius of the domain.

Problem 4 (Rotors of minimal volume.). *For P be a polygon (polyhedron) which admits rotors, solve*

$$\min\{|\Omega| : \Omega \subset P, \Omega \text{ is a rotor}\}.$$

The existence of rotors of minimal volume is guaranteed by Theorem 1 and properties 5, 7. Moreover, the fact that the Hausdorff limit of rotors is still a rotor comes from Property 2. It is enough to choose the normal directions orthogonal to the sides of the polygon (polyhedron) and observe the limit of the corresponding support functions evaluated at these directions.

In the following, functionals related to the volume and perimeter are considered, under width or diameter constraints.

Problem 5. *For $\gamma > 0$, minimize*

$$J_\gamma(\omega) = \gamma|\omega| - \mathcal{H}^{d-1}(\partial\omega)$$

for ω convex with diameter equal to 1.

This problem was presented at the workshop "New Trends in Shape Optimization" by J. Lamboley and the results are attributed to Henrot, Lamboley and Privat. The existence of solutions comes from Theorem 1 and Property 3.

The following problem was considered in [Oud13] and consists in minimizing the area under minimal width constraint.

Problem 6.

$$\min_{B\in\mathcal{K}} \mathcal{H}^2(\partial B), \text{ where } \mathcal{K} = \{B \subset \mathbb{R}^3 : B \text{ is convex and } p_B(\theta) + p_B(-\theta) \geq 1,\ \forall\theta \in \mathbb{S}^2\},$$

where p_B denotes the support function of the convex body B.

In [BB05, Proposition 2.4.3], it is proved that of two convex bodies $A, B \subset \mathbb{R}^d$ verify $A \subset B$ then $\mathcal{H}^{d-1}(\partial A) \leq \mathcal{H}^{d-1}(\partial B)$. Every body from $\mathcal{K}$ contains three mutually orthogonal segments of length ≥ 1. By convexity and the property above it is immediate to see that the volume of any body in $\mathcal{K}$ is at least $\frac{1}{8}$. Using the isoperimetric inequality, it can be seen that minimizing sequences exist and the existence of a solution comes from Theorem 1 and Property 6.

As an application for the inclusion constraint, the Cheeger set associated to some convex domains in dimension two and three is considered.

Problem 7 (Cheeger sets.). *The Cheeger set associated to a convex domain $D \subset \mathbb{R}^n$ is the solution of the following problem*

$$\min_{X\subset D} \frac{\mathcal{H}^{n-1}(\partial X)}{|X|},$$

where the minimum is taken over all convex sets X contained in D.

The Cheeger sets are extensively studied and it is not the objective to present the subject in detail here. In dimension two there is an efficient characterization which allows the analytical computation of Cheeger sets for a large class of domains [KLR06]. Computational approaches based on various methods were introduced in [LRO05], [CCP09], [CFM09] and [BBF18]. Note that in dimension two, the convexity of D implies the convexity of the optimal Cheeger set. In dimension three this is no longer the case. However, one can prove that there exists at least one convex optimum [LRO05]. Existence of Cheeger sets is a consequence of Theorem 1 and Properties 3, 5.

3.2 Convergence results

The numerical approach proposed in the following is to use a truncation of the spectral decomposition of the support function. Therefore, as underlined in [BH12] it is important to prove that increasing the number of non-zero coefficients N in the optimization gives a shape which converges to the solution of the original problem.

In the following, denote by

$$\mathcal{F}_N = \{p : p = \sum_{i=0}^{N} \alpha_i \phi_i, p \text{ is the support function of a convex body}\}.$$

This corresponds to the notation $\mathcal{F}_J$ used previously, with $J = \{0, 1, 2, ..., N\}$. Denote by $\mathcal{K}_N^d$ the class of convex sets in $\mathbb{R}^d$ whose support functions belong to $\mathcal{F}_N$. Property 7 proved in the previous section shows that $\mathcal{K}_N^d$ is closed under the Hausdorff metric. Therefore the existence of solutions can be shown for all problems recalled in the previous section by replacing the class of convex sets with $\mathcal{F}_N$.

An important question, which is not obvious at first sight, is whether a general convex body K can be approximated in the Hausdorff metric by convex bodies K_n with support functions in some $\mathcal{F}_{N_n}$. This is proved in [Sch14, Section 3.4]. Namely, the following property holds:

Property 8. *Let K be a convex body and $\varepsilon > 0$. Then there exists a positive integer $N_\varepsilon > 0$ and a convex set K_ε with support function in $\mathcal{F}_{N_\varepsilon}$ such that $d_H(K, K_\varepsilon) < \varepsilon$.*

Remark 1. *Following the remarks in [Sch14, p. 185], starting from a body of constant width K, the smoothing procedure preserves the constant width. Moreover, the approximation of K in $\mathcal{K}_{N_\varepsilon}^d$ is obtained by truncating the spectral decomposition of the regularized support function. This also preserves the constant width property, which is related to the fact that the coefficients of the even basis functions are zero. Therefore, if K is of constant width in the previous proposition, its approximation $K_\varepsilon \in \mathcal{F}_{N_\varepsilon}$ can also be chosen of the same constant width.*

In practice, however, it is often necessary to impose some other constraints, like fixed volume, area, minimal width, etc. Below we give another variant of this property for constraints of the form $\{\mathcal{C}(K) \geq c\}$ where $\mathcal{C}$ is a continuous function with respect to the Hausdorff metric which is homogeneous of degree $\alpha > 0$: $\mathcal{C}(\eta K) = \eta^\alpha \mathcal{C}(K)$ for $\eta > 0$. This includes many constraints of interest, like area, perimeter, minimal width, diameter, etc.

Property 9. *Let $\mathcal{C} : \mathcal{K}^n \to \mathbb{R}_+$ be a continuous functional, positively homogeneous of degree $\alpha > 0$. Let K be a convex body which satisfies $\mathcal{C}(K) \geq c$, for some fixed $c > 0$ and $\varepsilon > 0$. Then there exists a positive integer $N_\varepsilon > 0$ and a convex set K_ε with support function in $\mathcal{F}_{N_\varepsilon}$ such that $d_H(K, K_\varepsilon) < \varepsilon$ and $\mathcal{C}(K_\varepsilon) \geq c$.*

Proof: By the Property 8 there exists a sequence $K_n \to K$ in the Hausdorff metric such that $K_n \in \mathcal{K}_{N_n}^d$ for some $N_n > 0$. Since $\mathcal{C}$ is continuous it follows that $\mathcal{C}(K_n) \to \mathcal{C}(K)$. Define the new sets K_n' by $K_n' = \left(\frac{\mathcal{C}(K)}{\mathcal{C}(K_n)}\right)^{1/\alpha} K_n$. Then obviously $C(K_n') \geq c$ and

$$d_H(K_n', K) \leq d_H(K_n, K) + d_H(K_n, K_n').$$

Following the relation under between the Hausdorff distance and the support functions

$$d_H(K_n, K_n') = \|p_{K_n} - p_{K_n'}\|_\infty = \left|1 - \left(\frac{\mathcal{C}(K)}{\mathcal{C}(K_n)}\right)^{1/\alpha}\right| \|p_{K_n}\|_\infty \to 0 \text{ as } n \to \infty.$$

Therefore it is possible to approximate K in the Hausdorff metric with the sequence K_n' which also verifies the constraint $\mathcal{C}(K_n') \geq c$. □

Now we are ready to prove the following approximation result.

Theorem 2. *Let $\mathcal{G}$ be a continuous functional defined on the class of closed convex sets. Consider a constraint function $\mathcal{C}$ which is continuous for the Hausdorff metric and let $c > 0$. In the following $\mathcal{M}$ denotes one of the following: $\mathcal{K}^N$, $\{K \in \mathcal{K}_n : \mathcal{C}(K) \geq c\}$, or the set of sets in $\mathcal{K}^N$ of fixed constant width w. Denote by K_N a solution of*

$$\min_{K \in \mathcal{K}_N^d \cap \mathcal{M}} \mathcal{G}(K). \tag{11}$$

Then any converging subsequence of K_N converges in the Hausdorff metric to a solution K of

$$\min_{K \in \mathcal{K}^d \cap \mathcal{M}} \mathcal{G}(K). \tag{12}$$

Proof: First, let's note that the existence of solutions to problems (11) and (12) is immediate using Theorem 1, Property 7 the fact that $\mathcal{M}$ is closed and the continuity of $\mathcal{G}$.

Denote by K a solution of (12). By the results shown in Properties 8, 9 and Remark 1 there exists a sequence of convex sets $L_{N_n} \in \mathcal{K}_{N_n}^d \cap \mathcal{M}$ such that $L_{N_n} \to K$ in the Hausdorff metric.

In the following denote by K_N a solution of (11) for $N \geq 1$. It is obvious that $\mathcal{K}_{N_1}^d \subset \mathcal{K}_{N_2}^d \subset \mathcal{K}^d$ for $N_1 \leq N_2$. As an immediate consequence $\mathcal{G}(K_{N_1}) \geq \mathcal{G}(K_{N_2}) \geq \mathcal{G}(K)$ for $N_1 \leq N_2$. Therefore, the sequence $\{\mathcal{G}(K_N)\}_{N \geq 1}$ is non-increasing and bounded from below, which implies the existence of the limit $\lim_{N \to \infty} \mathcal{G}(K_N) = \ell \geq \mathcal{G}(K)$. By the optimality of K_N we have $\mathcal{G}(L_{N_n}) \geq \mathcal{G}(K_{N_n})$ and since $d_H(K, L_{K_n}) \to 0$, by the continuity of $\mathcal{G}$ we obtain

$$\mathcal{G}(K) = \lim_{n \to \infty} \mathcal{G}(L_{N_n}) \geq \lim_{n \to \infty} \mathcal{G}(K_{N_n}) = \ell \geq \mathcal{G}(K).$$

The inequality above implies that $\ell = \mathcal{G}(K)$. Furthermore, if a subsequence of $\{K_N\}_{N \geq 1}$ converges to K' in the Hausdorff metric it follows that $K' \in \mathcal{M}$ and $\mathcal{G}(K') = \ell = \min_{K \in \mathcal{K}^d \cap \mathcal{M}} \mathcal{G}(K)$. Therefore, every limit point for $\{K_N\}_{N \geq 1}$ in the Hausdorff metric is a minimizer of (12).

□

Theorem 2 motivates our numerical approach. In order to obtain an approximation of solutions of the shape optimization problems considered, a truncation of the spectral decomposition is used. The theoretical result states that the solutions of the finite dimensional minimization problems obtained converge to the solution of the original problem.

3.3 Shape derivatives for the Dirichlet Laplace eigenvalues

We have seen that functionals like volume or area have explicit formulas in terms of the coefficients in the Fourier or spherical harmonics decomposition. This gives straight forward formulas for gradients and Hessians which can be used in optimization algorithms. When the shape functional is more complex, direct formulas are not available. Below, we present how to pass from the Hadamard shape derivatives to derivatives in terms of coefficients of the decomposition into Fourier series or spherical harmonics.

The Hadamard shape derivative formula shows how a shape functional $\mathcal{F}(\omega)$ varies when considering some perturbation of the boundary given by a vector field V. One way to define this to consider the derivative of the functional $t \mapsto \mathcal{F}((\mathrm{Id} + tV)(\omega))$ at $t = 0$. Under mild regularity assumptions it can be proved that the shape derivative may be written as a linear functional depending on the normal component of V. For more details one could consult [HP18, Chapter 5]. In particular, in [HP18, Theorem 5.7.4], for the case of the eigenvalues of the Dirichlet-Laplace operator (10) the shape derivative is

$$\frac{\lambda_k'(\omega)}{dV} = -\int_{\partial\omega} \left(\frac{\partial u_k}{\partial n}\right)^2 V.n d\sigma,$$

as soon as eigenvalue $\lambda_k(\omega)$ is simple and the eigenfunction u_k is in $H^2(\omega)$. This is true in the particular case of convex sets. In the following, we suppose that the functional $\mathcal{F}(\omega)$ has a Hadamard shape derivative which can be written in the form

$$\frac{d\mathcal{F}(\omega)}{dV} = \int_{\partial\omega} fV.nd\sigma. \tag{13}$$

As underlined above, the case of Dirichlet-Laplace eigenvalues for convex domains, which interests us in the following enters in this framework.

3.3.1 Dimension 2

As already recalled in [BH12] a parametrization of the boundary of the convex width shape defined by the support function p is given by

$$\begin{cases} x(\theta) = p(\theta)\cos\theta - p'(\theta)\sin\theta \\ y(\theta) = p(\theta)\sin\theta + p'(\theta)\cos\theta. \end{cases}$$

and a straightforward computation gives

$$\begin{cases} x'(\theta) = -(p''(\theta) + p(\theta))\sin\theta \\ y'(\theta) = (p''(\theta) + p(\theta))\cos\theta. \end{cases}$$

Therefore the norm of the velocity vector is given by $\|(x'(\theta), y'(\theta))\| = p''(\theta) + p(\theta)$, which will help us compute the Jacobian when changing variables. Moreover, the normal to the point corresponding to parameter θ is simply $(\cos\theta, \sin\theta)$.

In order to compute the derivative of the functional with respect to the Fourier coefficients of the support function it is enough to transform the perturbation of the support function into a perturbation of the boundary and use the Hadamard formula. We summarize the derivative formulas below

1. *Derivative with respect to* a_0. The corresponding boundary perturbation is $V = (\cos\theta, \sin\theta)$ and the normal component is $V.n = 1$. Therefore the derivative is

$$\frac{\partial\mathcal{F}}{\partial a_0} = \int_{\partial\omega} fd\sigma = \int_0^{2\pi} f(p'' + p)d\sigma.$$

2. *Derivative with respect to* a_k. The corresponding boundary perturbation is

$$V = (\cos(k\theta)\cos\theta + k\sin(k\theta)\sin\theta, \cos(k\theta)\sin\theta - k\sin(k\theta)\cos\theta)$$

and the normal component is $V.n = \cos(k\theta)$. Therefore the derivative is

$$\frac{\partial\mathcal{F}}{\partial a_k} = \int_{\partial\omega} f\cos(k\theta)d\sigma = \int_0^{2\pi} f(\theta)\cos(k\theta)(p(\theta)'' + p(\theta))d\sigma.$$

3. *Derivative with respect to* b_k. The corresponding boundary perturbation is

$$V = (\sin(k\theta)\cos\theta - k\cos(k\theta)\sin\theta, \sin(k\theta)\sin\theta + k\cos(k\theta)\cos\theta)$$

and the normal component is $V.n = \sin(k\theta)$. Therefore the derivative is

$$\frac{\partial\mathcal{F}}{\partial b_k} = \int_{\partial\omega} f\sin(k\theta)d\sigma = \int_0^{2\pi} f(\theta)\sin(k\theta)(p(\theta)'' + p(\theta))d\sigma.$$

3.3.2 Dimension 3

We differentiate now a functional $\mathcal{F}(\omega)$ for 3D shapes parametrized using the coefficients of the spherical harmonic decomposition (17) of the support function. When considering a general perturbation of the support function $p \mapsto p+Y$ then, having in mind the boundary parametrization (6), we find that the boundary perturbation has the form

$$V = Y\mathbf{n} + \mathcal{P}(\theta,\phi)\mathbf{n}_\phi + \mathcal{Q}(\theta,\phi)\mathbf{n}_\psi.$$

Since the vectors $\mathbf{n}, \mathbf{n}_\phi$ and $\mathbf{n}_\psi$ are orthogonal, we find that the normal component is simply $V.n = Y$. Then, using the general Hadamard derivative formula (13) we find that the derivatives with respect to the coefficients in the spherical harmonic decomposition of the support function have the form

$$\frac{\partial \mathcal{F}}{\partial a_{l,m}} = \int_{\partial\omega} fY_{k,m}d\sigma = \int_{-\pi}^{\pi}\int_{0}^{\pi} f(\phi,\psi)Y_{l,m}(\phi,\psi)\text{Jac}(\psi,\phi)d\psi d\phi,$$

where $\text{Jac}(\psi,\phi)$ is the Jacobian function given by (9). Indeed, the Jacobian for such kind of surface integral is computed by $\text{Jac}(\phi,\psi) = \|\partial_\phi \mathbf{x}_p \times \partial_\psi \mathbf{x}_p\|$. Note that each of the vectors $\partial_\phi \mathbf{x}_p, \partial_\psi \mathbf{x}_p$ are orthogonal to the normal to the surface, which is exactly $\mathbf{n}$ given by (5). Therefore the Jacobian reduces to $\text{Jac}(\phi,\psi) = \mathbf{n}.(\partial_\phi \mathbf{x} \times \partial_\psi \mathbf{x})$ and by the expressions of the differentials of $\mathbf{x}$ in the tangent plane given by (8) we can conclude that $\text{Jac}(\phi,\psi)$ is indeed given by (9).

4 Numerical framework

When performing numerical simulations for shape optimization problems we need to express shapes using a finite number of parameters. Since, in our case, shapes will be parametrized using the support function, we would like to work with a sufficiently rich class of support functions which can be represented in a finite dimensional framework. The approach taken in our computations is to approximate one dimensional functions using a truncated Fourier series and two dimensional functions using a truncated expansion using spherical harmonics. Theoretical results shown in Section 3 further motivate this choice, as solutions obtained when working with truncated spectral decompositions converge to the solutions of the original problem as the number of non-zero coefficients considered goes to $+\infty$. This type of methods was already used in other contexts like [AF12], [Ost10], [AF16], [Ant16], [BH12]. Using such systems of orthogonal or orthonormal basis representations has further advantages which will be underlined below. Again, for the clarity of exposition, we divide the presentation following the dimension.

4.1 Dimension 2

We approximate the support function by a truncated Fourier series

$$p(\theta) = a_0 + \sum_{k=1}^{N} (a_k \cos k\theta + b_k \sin k\theta) \tag{14}$$

As stated in Section 2, in order for p to be the support function of a convex set in $\mathbb{R}^2$ we need to have $p''(\theta) + p(\theta) \geq 0$ for every $\theta \in [0, 2\pi)$. In [BH12] the authors provide an exact characterization of this condition in terms of the Fourier coefficients, involving concepts from semidefinite programming. In [Ant16] the author provides a discrete alternative of the convexity inequality which has the advantage of being linear in terms of the Fourier coefficients. We choose $\theta_m = 2\pi m/M,\ m = 1, 2, ..., M$ for some positive integer M and we impose the inequalities

$p(\theta_m) + p''(\theta_m) \geq 0$ for $m = 1, ..., M$. As already shown in [Ant16] we obtain the following system of linear inequalities

$$\begin{pmatrix} 1 & \alpha_{1,2} & \cdots & \alpha_{1,N} & \beta_{1,2} & \cdots & \beta_{1,N} \\ \vdots & \vdots & \ddots & \vdots & \vdots & \ddots & \vdots \\ 1 & \alpha_{M,2} & \cdots & \alpha_{M,N} & \beta_{M,2} & \cdots & \beta_{M,N} \end{pmatrix} \begin{pmatrix} a_0 \\ a_2 \\ \vdots \\ a_N \\ b_2 \\ \vdots \\ b_N \end{pmatrix} \geq \begin{pmatrix} 0 \\ \vdots \\ 0 \end{pmatrix} \tag{15}$$

where $\alpha_{m,n} = (1 - n^2)\cos(n\theta_m)$ and $\beta_{m,n} = (1 - n^2)\sin(n\theta_m)$.

Next we turn to the constant width condition $p(\theta) + p(\theta + \pi) = w$ for every $\theta \in [0, 2\pi)$. It is not difficult to see that this is equivalent to $a_0 = w/2$ and the coefficients of even index are zero: $a_{2k} = b_{2k} = 0,\ k = 1, ..., N$. This was already noted in [BH12].

An upper bound W on diameter can be introduced as a constraint for the support function as follows

$$p(\theta) + p(\theta + \pi) \leq W, \theta \in [0, 2\pi).$$

In the computations we consider a discrete version of the above inequality. Pick $\theta_m = 2\pi m/M_d$, $m = 1, 2, ..., M_d$ for some positive integer M_d and impose the following linear inequalities

$$p(\theta_m) + p(\theta_m + \pi) \leq W,\ m = 1, ..., M_d. \tag{16}$$

It is not difficult to see that (16) can be generalized to the case where W also varies with θ. In order to impose a lower bound on the diameter it is enough to pick one direction θ and use the constraint

$$p(\theta) + p(\theta + \pi) \geq w.$$

It is also possible to consider variable lower and upper bounds on the width of the body which depend on θ.

Let us now recall the formulas for the area and perimeter of a two dimensional shape in terms of the Fourier coefficients of the support function. The perimeter is simply equal to $P(p) = 2\pi a_0$, which is linear in terms of the Fourier coefficients. As already stated in [BH12] the area of a convex shape having support function p with the Fourier decomposition (14) is given by

$$A(p) = \pi a_0^2 + \pi/2 \sum_{i=1}^{N} (1 - k^2)(a_k^2 + b_k^2).$$

Note that a_1 and b_1 do not contribute to the area computations as modifying a_1, b_1 only leads to translations of the shape defined by p.

4.2 Dimension 3

In [AF16] the authors parametrized three dimensional domains by their radial function using spherical harmonics. In our case we consider support function parametrized by a finite number of spherical harmonics

$$p(\phi, \psi) = \sum_{l=0}^{N} \sum_{m=-l}^{l} a_{l,m} Y_l^m(\psi, \phi) \tag{17}$$

for a given positive integer N. The spherical harmonics are defined by

$$Y_l^m(\psi, \phi) = \begin{cases} \sqrt{2} C_l^m \cos(m\phi) P_l^m(\cos\psi) & \text{if } m > 0 \\ C_l^0 P_l^0(\cos\psi) & \text{if } m = 0 \\ \sqrt{2} C_l^m \sin(-m\phi) P_l^{-m}(\cos\psi) & \text{if } m < 0, \end{cases}$$

where P_l^m are the associated Legendre polynomials and

$$C_l^m = \sqrt{\frac{(2l+1)(l-|m|)!}{4\pi(l+|m|)!}}$$

are normalization constants.

The convexity constraint is imposed by considering a discrete version of (9). Indeed, we construct a family of M_d evenly distributed points on the unit sphere, for example like described in [Ant11, Section 3]. We denote by (ϕ_i, ψ_i) $i = 1, ..., M_d$ the corresponding angles given by the parametrization (5). We impose that the convexity condition (9) is satisfied at points given by (ϕ_i, ψ_i), $i = 1, ..., M_d$. As in the two dimensional case, width inequality constraints can be handled in a similar way, by imposing inequalities of the type

$$w_i \leq p(u_i) + p(-u_i) \leq W_i$$

at points $u_i = (\phi_i, \psi_i)$ (see (5)).

The constant width condition is $p(u) + p(-u) = w$. This simply means that in the decomposition (17) we only have odd spherical harmonics, except the constant term. This corresponds to considering only spherical harmonics for which the index l is odd. In the following, we note with h the part of the support function containing the non-constant terms. Equivalently $h = p - \frac{1}{4\pi}\int_{\mathbb{S}^2} p d\sigma$.

The area and volume of a convex body of constant width w in dimension three can be computed explicitly in terms of the spherical harmonics coefficients. Indeed, in [AG11, Theorem 2], the following formulas are provided:

$$V = \frac{\pi}{6}w^3 - \frac{w}{2}\mathcal{E}(h) \tag{18}$$

$$A = \pi w^2 - \mathcal{E}(h). \tag{19}$$

where $\mathcal{E}(h) = \displaystyle\int_{\mathbb{S}^2} \left(\frac{1}{2}|\nabla_\tau h|^2 - h^2\right) dA$. The formulas in [AG11] are for a body of constant width $2w$, which we transformed so that they correspond to a body of width w. Using the fact that the spherical harmonics Y_l^m are chosen to be an orthonormal family we can see that, in fact $\mathcal{E}(p)$ can be computed explicitly in terms of the coefficients $a_{l,m}$ and the eigenvalues $\lambda_{l,m}$ corresponding to the spherical harmonics $Y_{l,m}$:

$$\mathcal{E}(h) = \sum_{l=1}^{N}\sum_{m=-l}^{l}\left(\frac{\lambda_{l,m}}{2} - 1\right)a_{l,m}^2. \tag{20}$$

Therefore, when dealing with bodies of constant width, the volume and the area have explicit formulas in terms of the coefficients $a_{l,m}$ of the decomposition (17).

We note that it is also possible to compute explicitly the area of a general convex body, using the coefficients of the support functions. Indeed, Lemma 1 from [AG11, Section 5] is valid for general support functions h, not only those corresponding to a constant width body. Therefore the area of a convex body B is also given by (19), where $w = 2a_{0,0}Y_0^0$. Also following the results stated in [AG11] it should also be possible to compute the volume explicitly using the Gaunt coefficients involving integrals on the sphere of products of three spherical harmonics. In our computations, for general bodies parametrized using their support function, we used an alternative way to compute the volume. Using the divergence theorem, we can compute the volume of a convex body ω as the integral on $\partial\omega$ of a vector field V with divergence equal to one. For simplicity we choose $V = \frac{1}{3}\mathbf{x} = \frac{1}{3}(x, y, z)$ and we integrate $V.n$ on $\partial\omega$. One may note that since we are working with bodies parametrized by their support function, the quantity $V.n$ computed at $x_0 \in \partial\omega$ is the value of the support function at x_0: $\mathbf{x}.n(x_0) = p(x_0)$.

4.3 Visualization of results

It may be useful to underline how the results are visualized. Following the aspects presented in previous sections, we use a family of coefficients which parametrize a spectral decomposition of the support function. The variables in the optimization algorithm, and therefore, the output obtained will contain such coefficients. Given a family of Fourier coefficients (spherical harmonics coefficients) it is possible to evaluate the support function and its derivatives at any point in the unit circle (unit sphere in dimension three).

Once the values of the support function and its derivatives are known at a family of discretization points it is possible to use the formula (4) in dimension two (formula (6) in dimension three) in order to find the associated points on the boundary of the domain. When such a family of points is known a simple contour plot is made in dimension two. In dimension three, the Matlab command `convhull` is used to generate a triangulation of the surface bounding the convex body. Then the command `patch` allows us to plot the surface.

5 Computation of the Dirichlet-Laplace eigenvalues

The Dirichlet-Laplace eigenvalue problem (10) is solved using the Method of Fundamental Solutions (MFS) [Kar01, AA13]. We consider a fundamental solution of the Helmholtz equation,

$$\Phi_\lambda(x) = \frac{i}{4} H_0^{(1)}(\sqrt{\lambda}\,|x|) \tag{21}$$

and

$$\Phi_\lambda(x) = \frac{e^{i\sqrt{\lambda}|x|}}{4\pi\,|x|}, \tag{22}$$

respectively for 2D and 3D cases, where $H_0^{(1)}$ denotes the first Hankel function. For a fixed value of λ, the MFS approximation is a linear combination

$$\sum_{j=1}^{m} \alpha_j \Phi_\lambda(\cdot - y_j), \tag{23}$$

where the source points y_j are placed on an admissible source set, for instance the boundary of a bounded open set $\hat{\omega} \supset \bar{\omega}$, with $\partial\hat{\omega}$ surrounding $\partial\omega$. By construction, the MFS approximation satisfies the PDE of the eigenvalue problem (10) and we can just focus on the approximation of the boundary conditions, which can be justified by density results (e.g. [AA13]).

Next, we give a brief description of the numerical procedure for calculating the Dirichlet-Laplace eigenvalues. We define two sets of points $W = \{w_i,\ i = 1, ..., n\}$ and $X = \{x_i,\ i = 1, ..., m\}$, almost uniformly distributed on the boundary $\partial\omega$, with $n < m$ and the set of source points, $Y = \{w_i + \alpha n_i,,\ i = 1, ..., n\}$ where α is a positive parameter and n_i is the unitary outward normal vector at the point w_i. We consider also some interior points z_i, $i = 1, ..., p$ with $(p < m)$ randomly chosen in ω and used the Betcke-Trefethen subspace angle [BT05]. After defining the matrices

$$\mathbf{M}_1(\lambda) = \left[\Phi_\lambda(x_i - y_j)\right]_{m\times n}, \tag{24}$$

$$\mathbf{M}_2(\lambda) = \left[\Phi_\lambda(z_i - y_j)\right]_{p\times n} \tag{25}$$

and $\mathbf{A}(\lambda) = \begin{bmatrix} \mathbf{M}_1(\lambda) \\ \mathbf{M}_2(\lambda) \end{bmatrix}$ we compute the QR factorization

$$\mathbf{A}(\lambda) = \begin{bmatrix} \mathbf{Q}_1(\lambda) \\ \mathbf{Q}_2(\lambda) \end{bmatrix} \mathbf{R}$$

and calculate the smallest singular value of the block $\mathbf{Q}_1(\lambda)$, which will be denoted by $\sigma_1(\lambda)$. The approximations for the Dirichlet-Laplace eigenvalues are the local minima λ, for which $\sigma_1(\lambda) \approx 0$.

6 Applications

This section shows how the proposed numerical framework applies to the various problems presented in Section 3. In all the simulations with 2D domains, we considered $N = 300$ for defining the support function in (14) and $M_2 = 2000$ directions to impose the convexity constraint, while the numerical results with 3D geometries were obtained with $N \leq 28$ in (17) and $M_3 = 5000$. In general, the number of discretization points where we consider the convexity constraints should be chosen such that the highest order modes considered in the decomposition of the support function cannot oscillate much between two neighboring points.

The Matlab `fmincon` function is used in each of the various problems shown below with the `interior-point` algorithm. As shown in previous sections, all constraints on the shapes are transformed into algebraic constraints on the coefficients of a spectral decomposition. The full functionality of `fmincon` is used in order to handle: linear equality/inequality constraints and non-linear constraints. The gradient of the functional and the constraints is computed and is always used in the algorithm. When possible, the Hessian matrix is also computed, and in all the other computations a LBFGS approximation is used.

6.1 Convexity constraint – the Dirichlet-Laplace eigenvalues

We illustrate the behavior of our numerical framework by studying a classical shape optimization problem related to the eigenvalues of the Dirichlet-Laplace operator under convexity constraints defined in Problem 1. Two basic properties of these eigenvalues are the monotonicity with respect to inclusion and the scaling property:

$$\omega_1 \subset \omega_2 \Rightarrow \lambda_k(\omega_1) \geq \lambda_k(\omega_2) \text{ and } \lambda_k(t\omega) = \frac{1}{t^2}\lambda_k(\omega)$$

The theoretical and numerical study of minimization problems of the form

$$\min_{\omega \in \mathcal{A}} \lambda_k(\omega)$$

gained a lot of interest in the recent years. Various problems were considered, like the optimization of eigenvalues under volume constraint [Buc12], [MP13], the optimization under perimeter constraint [DPV14] and recently, the minimization under diamenter constraint [BHL17]. For many of the problems considered, explicit solutions are not known, therefore various works, like [Oud04], [AF12], [AF16] deal with the optimization of the eigenvalues for volume and perimeter constraints. Such constraints can be naturally incorporated in the functional, in view of the behaviour of the eigenvalue with respect to scaling, and therefore unconstrained optimization algorithms based on information given by the shape derivative are successfully used in practice.

The optimization of eigenvalues under convexity constraints poses additional difficulties. These are underlined in the study of the second eigenvalue

$$\min_{|\omega|=1,\ \omega \text{ convex}} \lambda_2(\omega). \tag{26}$$

This problem is studied in [HO03] and the authors show that the optimizer is not the convex-hull of two tangent disks, as conjectured before. Moreover, the authors of [HO03] show that the boundary of the optimal set cannot contain arcs of circles. In the same publication the authors propose an algorithm for finding numerically the minimizer of (26), by using a penalization of the difference between the volume of the shape and the volume of its convex hull. A more precise, parametric search for the minimum was done in [AH11], giving an optimal numerical value of $\lambda_2(\omega) = 37.987$.

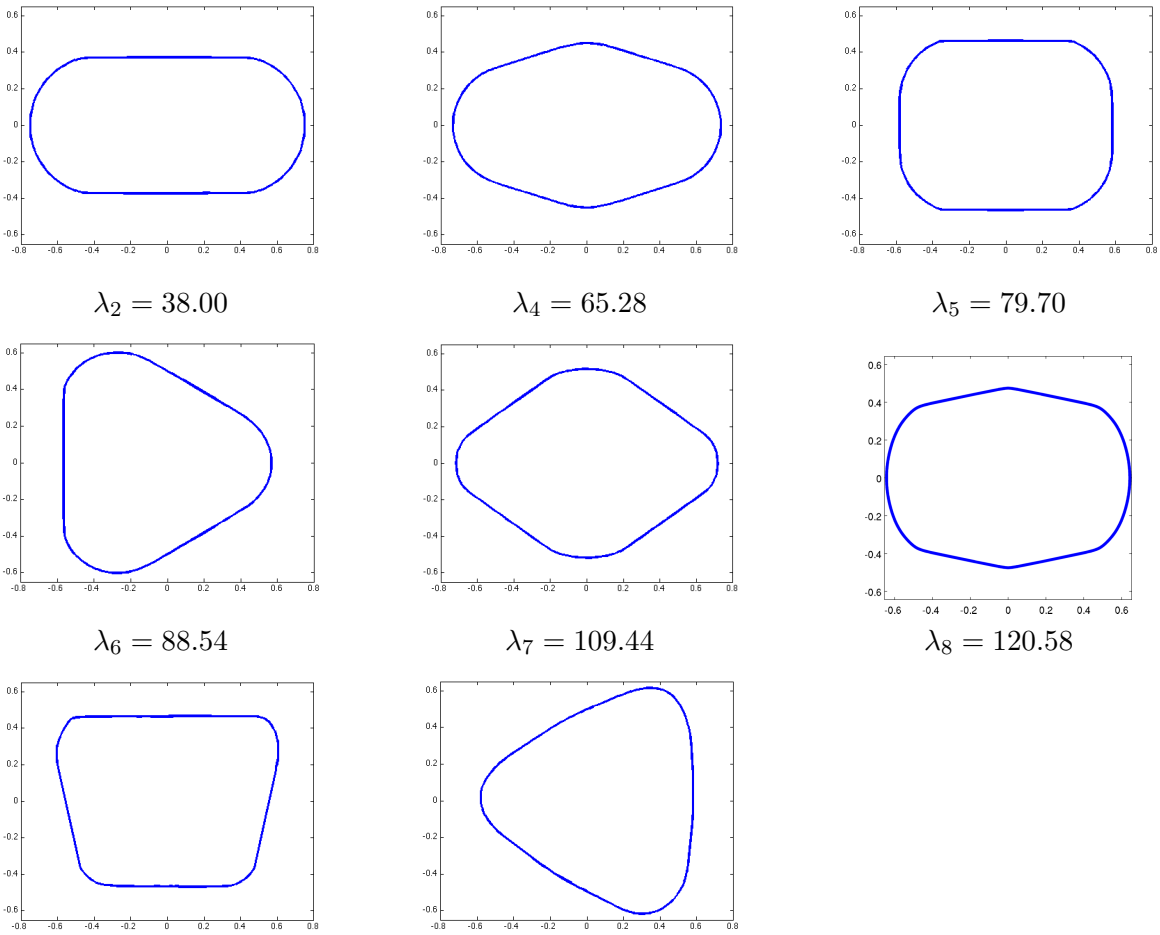

Figure 1: Minimization of the eigenvalues of the Dirichlet-Laplace operator under convexity and volume constraints in dimension two. The numerical minimizer of the third eigenvalue is the disk, even without imposing the convexity constraint.

In the following we show results obtained using the numerical framework proposed in previous section, in order to deal with the convexity constraint with the aid of a Fourier series decomposition of the support function. This requires no additional work regarding the functional we want to optimize. For the optimization we use Matlab's `fmincon` routine, with linear inequality constraints given by the discrete convexity constraint equations shown in (15). Results are summarized in Figure 1. Our numerical results support the well known conjecture (see for example [Oud04],[AF12]) that the disk shall be the minimizer of the third eigenvalue, even without imposing convexity constraint. Note that the values presented in Figure 1 were obtained rounding up the optimal values obtained with our numerical algorithm and are thus upper bounds for the optimal values.

We compute the eigenvalues and corresponding eigenfunctions using the method of fundamental solution recalled in Section 5. The derivative with respect to every Fourier coefficient in the parametrization is computed using results shown in Section 3.3.

The numerical discretization we consider in Section 4.2 allows us to perform the same computation in dimension 3, with no additional difficulty. We present these results in Figure 2 for $k \in \{2, 3, 5, 6, 7, 8, 10\}$. For $k \in \{4, 9\}$ we obtain balls as minimizers, which is natural, as numerical results show that considering a volume constraint alone we find that the ball minimizes λ_4 and λ_9 in $3D$. One may notice that as in the two dimensional case, studied in [HO03], there are

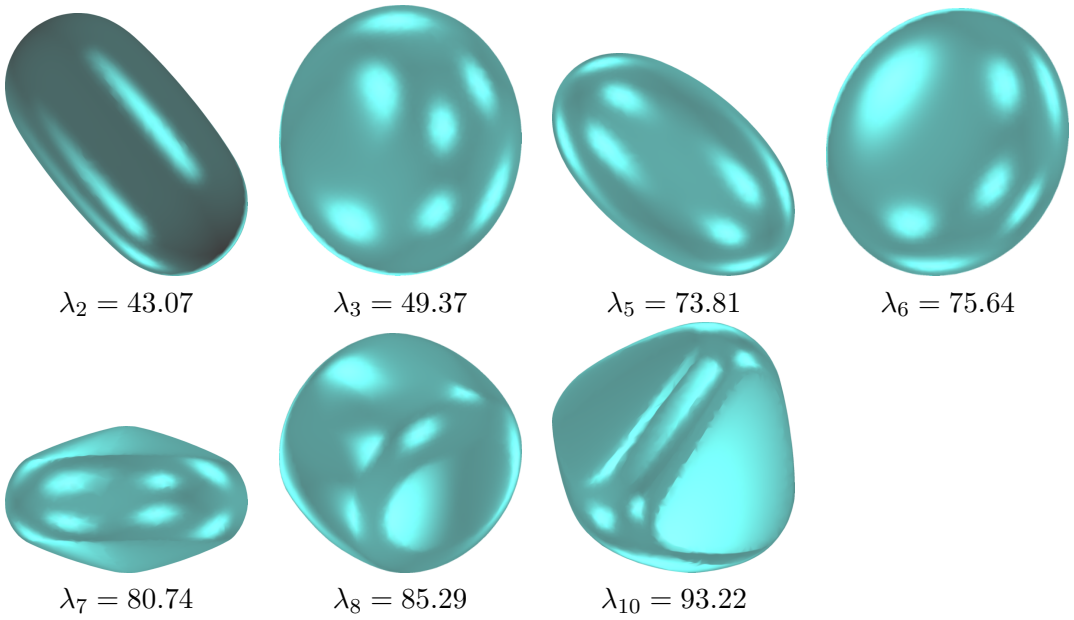

Figure 2: Optimization of eigenvalues under fixed volume and convexity constraint in 3D. For $k \in \{4, 9\}$ the ball is a numerical minimizer for λ_k at fixed volume even without imposing the convexity constraint.

parts of the numerical optimizers which seem to have at least one of the principal curvatures which vanish. This behavior could be a consequence of the following facts:

- ⋆ minimizers of the eigenvalues with volume constraint tend to be non-convex, in general
- ⋆ the eigenvalues are decreasing with respect to the inclusion of domains, so the eigenvalues of the convex hull are always lower than the eigenvalues of the actual shapes

6.2 Constant width constraint

We use the parametrizations presented in Section 4 in order to numerically solve shape optimization problems in the class of shapes of constant width. We show how our algorithm behaves for Problem 3, when minimizing the area in dimension two obtaining the Reuleaux triangle and the volume in dimension three, confirming the Meissner conjecture. We also show how the Dirichlet-Laplace eigenvalues behave under diameter constraint in dimension three (Problem 2).

As already underlined in Section 4, the parametrization of shapes using the Fourier or spherical harmonics coefficients has multiple advantages in this context. In order to impose the constant width constraint, it is enough to fix the first coefficient and make all other even-index coefficients equal to zero. This corresponds to an optimization problem in terms of the odd-index coefficients. It is also necessary to impose the convexity constraint, which we do in the discrete sense, by adding a set of linear inequality constraints (15). Another advantage is the fact that the area (volume) has an explicit quadratic expression in terms of the Fourier (spherical harmonics) coefficients corresponding to the support function. Therefore, in this case we may compute the functional, its gradient and the corresponding Hessian matrix explicitly, leading to quickly converging numerical algorithms.

Concerning Problem 3, we start by showing the behavior of the algorithm when optimizing the area under constant width in dimension two. Given the Fourier decomposition of the support function (14) the area is equal to

$$A(p) = \pi a_0^2 + \pi/2 \sum_{i=1}^{N} (1 - k^2)(a_k^2 + b_k^2).$$

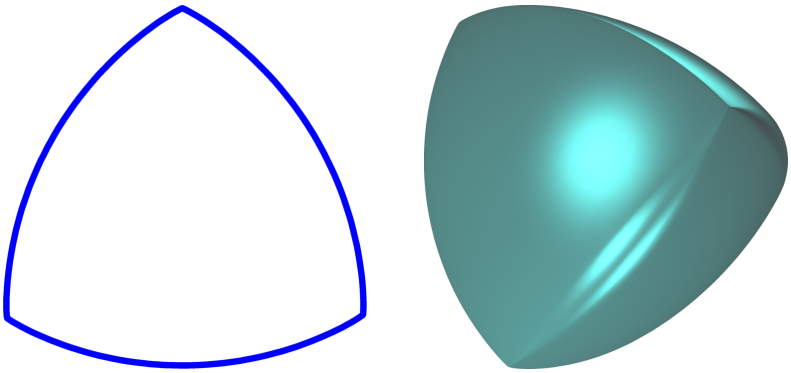

Figure 3: Minimization of area and volume under constant width constraint.

The constraints imposed on the Fourier coefficients are the following:

- $a_0 = w/2$, where w is the desired constant width
- $a_{2k} = b_{2k} = 0$ for $k \geq 1$.
- the Fourier coefficients verify the discrete convexity constraint (15)

Therefore, we obtain the following constrained quadratic problem which approximates the shape minimizing the area under constant width constraint:

$$\min \left(\pi \frac{w^2}{4} + \frac{\pi}{2} \sum_{k=0}^{N/2} (1 - (2k+1)^2)(a_{2k+1}^2 + b_{2k+1}^2) \right) \tag{27}$$

under the linear discrete convexity constraint (15). We solve (27) using `fmincon` in Matlab. The optimization algorithm is `interior-point` with an explicit gradient and Hessian computation. The result is given in Figure 3. The minimal value for the area obtained with our algorithm, for $N = 250$, corresponding to 501 Fourier coefficients and width $w = 2$ was 2.8196 which is slightly larger than but very close to the explicit area of the Reuleaux triangle of width 2 which is equal to $2(\pi - \sqrt{3}) = 2.8191$.

The minimization of the volume under constant width constraint in dimension three is a famous open problem. The conjectured optimizer is a Reuleaux tetrahedron with three rounded edges. There are two configurations, with the same volume, the difference being in the position of the rounded edges: all starting from one vertex or forming a triangle. These shapes are called Meissner's bodies. Various works deal with the analysis of 3D shapes of constant width which minimize the volume. Among these we cite [KW11], which presents many aspects related to the Meissner bodies and why they are conjectured to be optimal. It is mentioned that in [Mü09] the author generates a million random three dimensional bodies of constant width, using techniques from [LRO07]. Among these many bodies of constant width, none had a smaller volume than the ones of Meissner. In [Oud13] the local optimality of the Meissner's body was verified using an optimization procedure for a different parametrization of constant width shapes.

The approach we present below allows us to obtain the Meissner bodies as results of a direct optimization procedure, starting from random initializations. The formulas (18) and (20) allow us to write the volume as a quadratic expression of the coefficients of the spherical harmonics decomposition (17). The constant width condition is imposed by fixing the first coefficient and considering only odd spherical harmonics in the decomposition. The convexity condition is achieved by using a discrete version of (9). We note that in this case the convexity condition is non-linear, but it is explicit enough such that we may compute the gradient of the constraint. In this way, the minimization of the volume under constant width condition in dimension three becomes a constrained optimization problem of a quadratic functional with non-linear quadratic constraints. We implement this using `fmincon` in Matlab, using an

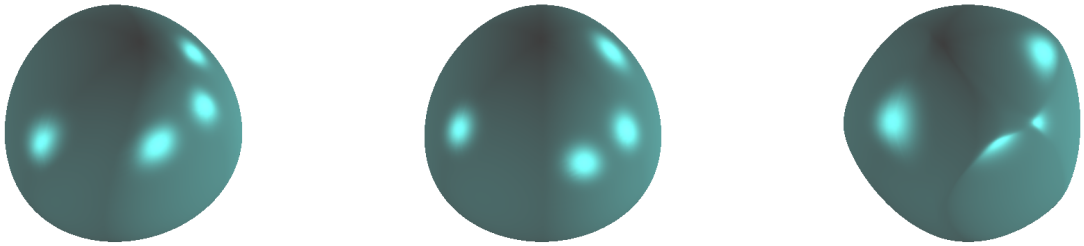

$\lambda_{10} = 39.41$
$\lambda_{10}(\bigcirc) = 39.48$

$\lambda_{46} = 88.80$
$\lambda_{46}(\bigcirc) = 88.83$

$\lambda_{99} = 156.14$
$\lambda_{99}(\bigcirc) = 157.92$

Figure 4: Minimization of the eigenvalues λ_k, with $k \in \{10, 46, 99\}$ under fixed width in 3D.

`interior-point` algorithm with objective gradient and Hessian activated. For unit width, in view of [KW11], the Meissner bodies have volume equal to

$$V_M = \pi \left(\frac{2}{3} - \frac{\sqrt{3}}{4} \cdot \arccos \frac{1}{3} \right) = 0.419860$$

In our computation, using 402 spherical harmonics, which means using Legendre polynomials up to degree 28, we obtain the shape represented in Figure 3, with volume 0.4224. Even if the shape we obtain strongly resembles Meissner's body, its volume is about 0.6% larger than V_M presented above. This may be due to the fact that singularities in the surface of the Meissner bodies are not sufficiently well approximated using the number of spherical harmonics stated above. Starting from different random initial coefficients we always arrive at shapes which are close to one of the two Meissner bodies [KW11].

In order to underline the strength of our algorithm, we also study the minimization of the Dirichlet-Laplace eigenvalues under diameter constraint in dimension 3 (Problem 2). This shows that our algorithm is not restricted to quadratic functionals (as in [BH12]), but may well work in more general cases. We already gave a brief definition of the eigenvalues in (10). The two dimensional case was treated in [BHL17]. The monotonicity property of the eigenvalues and the fact that every convex domain is contained in a constant width set with the same diameter makes that minimizers of $\lambda_k(\omega)$ under diameter constraint must be shapes of constant width. What makes the width constraint different from other constraints, like the perimeter or the volume, is the fact that the disk appears more often as a local optimizer in computations made in [BHL17]. In fact the precise list of indexes k for which the disk is a local minimizer for $\lambda_k(\omega)$ under width constraint in dimension two was given in [BHL17].

In our computations in dimension 3, we impose the constant width and convexity constraints just like in the case presented above (minimization of the volume). The difference is that the functional to be optimized is more computationally challenging. We only use gradient information in order to perform the optimization. As before, we use `fmincon` in Matlab with the `interior-point` option. In our computations we observe a similar behavior as in the two dimensional case. The ball appears often as a minimizer, but as observed in the two dimensional case in [BHL17], we expect that this only happens for finitely many indexes k. Notable exceptions are the indexes for which the corresponding eigenvalue is simple. In Figure 4 we present the non-trivial shapes of constant width obtained with our algorithm for $k \in \{10, 46, 99\}$, which are the three smallest indexes for which the corresponding eigenvalue of the ball is simple. For a comparison we present also in Figure 4 the eigenvalue obtained for the ball. As in the study of the two dimensional case found in [BHL17], one could investigate the local minimality of the eigenvalues of the Dirichlet-Laplace operator on the ball in the class of constant width bodies.

6.3 Rotors

As underlined in Section 3, for some convex domains P there exist convex shapes ω which can rotate inside P while touching all its sides (or faces in dimension three). Therefore, it makes sense to consider the problem of finding such rotors of minimal volume. Theoretical aspects are recalled in the definition of Problem 4 and numerical computations for the two dimensional case are presented in [BH12]. In dimension three there exist rotors for the cube (constant width bodies), the regular tetrahedron and the regular octahedron. A characterization of rotors in terms of the coefficients of the decomposition of the support function can be found in [Gol60]. More precisely we have the following:

- In dimension two every regular polygon admits non-circular rotors. If the regular polygon has n sides, $n \geq 3$, then only the coefficients for which the index has the form $nq \pm 1$ are non-zero, where q is a positive integer.
- the rotors in a cube are bodies of constant width
- rotors in a regular tetrahedron we only have non-zero coefficients for the spherical harmonics of index $0, 1, 2$ and 5
- rotors in a regular octahedron the non-zero coefficients are of index $0, 1$ and 5.

The constant term in the spectral decomposition of the support function of a rotor corresponds to the inradius of the domain.

Using the parametrization based on the support function we compute numerically rotors of minimal area in dimension two and rotors of minimal volume in dimension three. Computations of optimal rotors in dimension two were also made in [BH12], while the computations in dimension three are new, up to the authors' knowledge. We note that rotors of maximal area and volume are the inscribed disc and the inscribed ball, respectively. Some results are depicted in Figures 5 and 6. We do not repeat the numerical framework, since we used the same algorithm as in the case of constant-width constraint computations made in Section 6.2. In each case we consider an optimization problem depending only on the non-zero coefficients describing the rotors and we impose discrete convexity constraints like described in Section 6.1. The computations presented in Figure 6 are made for solids with inradius equal to 0.5, corresponding to an inscribed ball of diameter 1. Compared to the volume of the sphere B with unit diameter which is equal to $\pi/6 = 0.5236$ the minimal volume found numerically of a rotor in the tetrahedron and the octahedron circumscribed to the same ball B are 0.3936 and 0.5041. Numerical minimizers for the tetrahedron and octahedron seem to be symmetric under a rotation of angle $2\pi/5$. This is due to the fact that the only coefficients which may change the geometry of the rotors correspond to the spherical harmonics of order 2 or of order 5. We recall that changing coefficients for spherical harmonics of order 1 correspond to translations. In particular, when searching for minimal rotors in the tetrahedron using only spherical harmonics of order 1 and 2 we get a radially symmetric minimizer of volume 0.4024 which is slightly larger than the result including spherical harmonics of order 5.

We note that when taking the midpoints of the edges of the regular tetrahedron we obtain a regular octahedron with the same inradius. Therefore rotors in the octahedron are also rotors for the tetrahedron which was already apparent from the characterization using the spherical harmonic coefficients.

6.4 Diameter constraint

In this section we show how diameter inequality constraints could be handled with our numerical framework. We start with a two dimensional example. As already shown in equation (16), diameter bounds in the direction given by θ can be imposed using inequality constraints for $p(\theta) + p(\pi + \theta)$ and as in the case of the convexity constraint, we choose to impose the diameter inequality constraints on a sufficiently dense discrete family of directions. Next, we show how the algorithm works on some concrete examples.

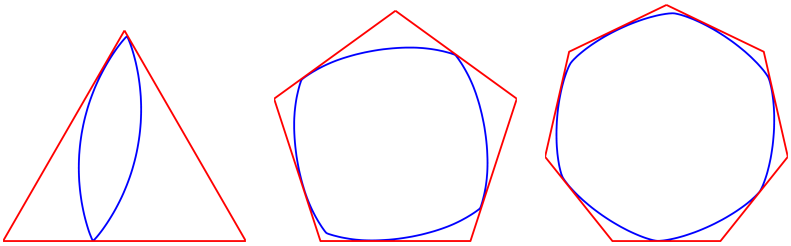

Figure 5: Examples of minimal area rotors in dimension two.

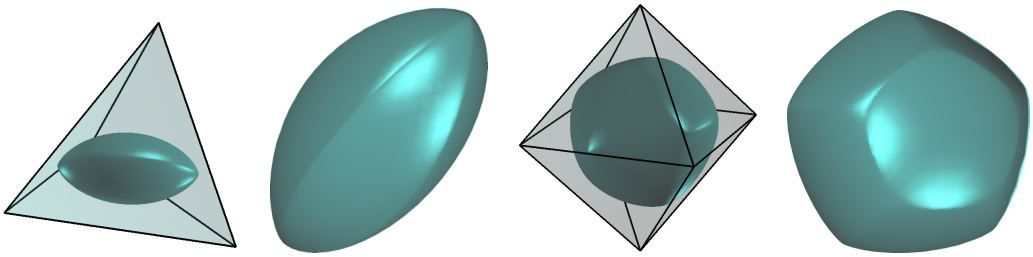

Figure 6: Minimal volume rotors in the regular tetrahedron and the regular octahedron. Volume of the inscribed sphere: 0.5236. Volume of the rotors: tetrahedron 0.3936, octahedron 0.5041.

First, consider Problem 5, where the functional $J_\gamma(\omega) = \gamma|\omega| - \mathcal{H}^{d-1}(\partial\omega)$ is minimized when ω has diameter equal to 1. It can be observed that this functional behaves differently for certain ranges of the parameter γ.

- if $\gamma \leq 0.5$ then the Reuleaux triangle is the optimizer
- if $\gamma \in (0.5, \frac{4}{\sqrt{3}})$ then the minimizer is a polygon
- if $\gamma > \frac{4}{\sqrt{3}}$ then the minimizer is the segment

We show below how our algorithm behaves when searching numerically for the minimizers of J_γ for various values of γ. Let's notice first, that optimizing in the class of shapes of diameter equal to 1 is the same as optimizing in the class of shapes with diameter at most 1. Indeed, if we have a convex shape of diameter less than 1 then one can slightly elongate the shape along a direction decreasing the area and increasing the perimeter. Therefore we consider the minimization of J_γ for convex shapes with diameter at most 1.

We implement an algorithm minimizing J_γ in dimension two. As before, we represent the shape ω using its support function and we decompose the support function in its Fourier series. In this case we use 201 coefficients in the Fourier expansion. The convexity condition and the diameter constraint inequalities are imposed using 1000 equidistant points in $[0, 2\pi]$. Since the area and the perimeter both have explicit expressions in terms of the Fourier coefficients, we may compute explicitly the gradient and the Hessian and use a second order optimization algorithm. Numerical results obtained for various values of γ are shown in Figure 7. Note that the algorithm is capable of numerically approximating optimal shape which are polygons, as expected for $\gamma > 0.5$. Singularities are well captured when considering a large enough number of Fourier coefficients and a dense enough family of points where we impose the convexity and diameter constraints.

Another example, considered in [Oud13] is Problem 6 where the area of a three-dimensional convex body is minimized under a minimal width constraint. The minimal width constraint is expressed in terms of the support function by $p(\theta) + p(-\theta) \geq 1$, for every $\theta \in \mathbb{S}^2$.

As underlined in Section 4.2, the diameter bounds can be imposed in an approximate manner at a finite family of points uniformly distributed on the sphere. This is done in the same way as the discrete convexity condition. Therefore, these bounds on the diameter correspond

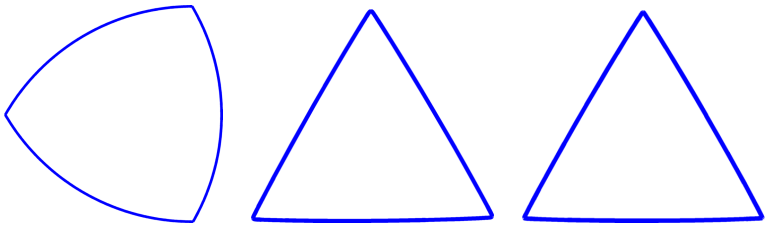

Figure 7: Minimization of J_γ for $\gamma \in \{0.4, 0.6, 1\}$

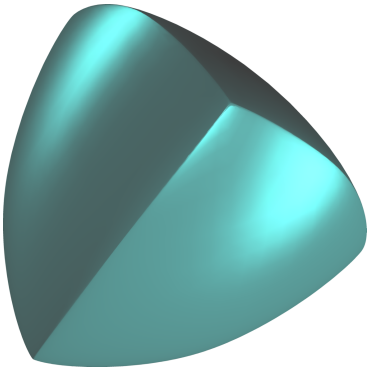

Figure 8: Optimization under diameter bounds in dimension three. Minimization of the area for shapes having width at least 1. The minimal area found by our algorithm is 2.9154.

to a set of linear inequality constraints. In Figure 8 we present the result given by the algorithm. The shape resembles the optimizer given in [Oud13] and the value of the functional is slightly improved. In the computations we used 2000 points for the discrete convexity condition and 1000 pairs of opposite diametral points for computing the discrete diameter conditions. We used 250 spherical harmonics in the decomposition of the support function. The computation of the area was done explicitly starting from the spherical harmonics coefficients, as shown in Section 4.2. The minimal area obtained with our algorithm is 2.9154 which is slightly lower than 2.9249, the value of the minimal area in the result presented by Oudet in [Oud13].

6.5 Inclusion constraint

In this subsection we show how to impose inclusion constraints for shape optimization problems. As recalled in Section 2, two convex bodies B_1, B_2 in $\mathbb{R}^n$, with support functions p_{B_1}, p_{B_2}, respectively satisfy the inclusion constraint $B_1 \subset B_2$ if and only if the support functions verify

$$p_{B_1}(\theta) \leq p_{B_2}(\theta) \text{ for every } \theta \in \mathbb{S}^{n-1}. \tag{28}$$

As in the case of the convexity and diameter constraints, we impose (28) on a sufficiently dense discrete set of $\mathbb{S}^{n-1}$. In dimension three, when dealing with Cheeger sets for polyhedra, it is enough to impose the inclusion constraints only for directions which are normals to the faces of the polyhedron. This simplifies the optimization algorithm by decreasing the number of constraints.

An example of classical context involving convexity and inclusion constraints is the case of the Cheeger sets. The theoretical formulation is given in Problem 7. The Cheeger sets fo some set D minimize the ratio perimeter/area for convex subsets of D. The ratio perimeter/area can be computed and optimized using our algorithm. We consider the constraints

$$X \text{ convex and } X \subset D,$$

which are discretized as linear inequalities regarding the coefficients of the spectral decomposition of the support function of the variable set X. Some examples of computation of Cheeger

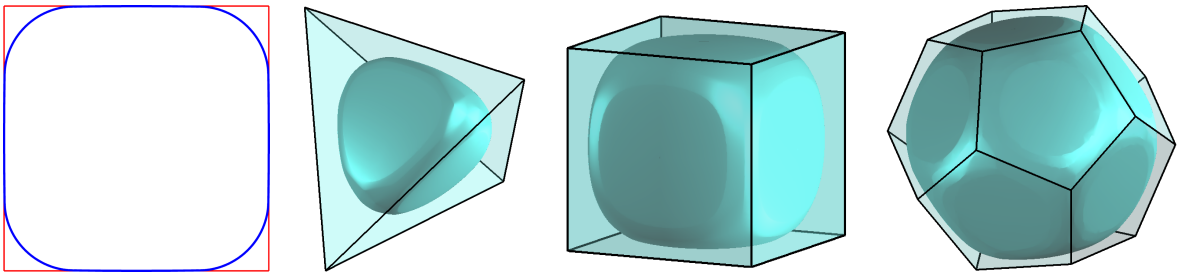

Figure 9: Computation of Cheeger sets by optimizing the ratio perimeter/volume under convexity and inclusion constraints.

sets for the square in the plane and for the regular tetrahedron, the cube and the regular dodecahedron in dimension three are shown in Figure 9.

7 Conclusions

In this work, the properties of the support function are used to deal numerically with various non-standard and non-local constraints in shape optimization problems. The spectral decomposition of the support function using Fourier series in dimension two and spherical harmonics in dimension three is particularly well suited in order to discretize convexity, constant-width, diameter and inclusion constraints. The numerical tests use standard tools readily available in optimization software like quasi-Newton or Newton methods with linear or non-linear constraints and cover a wide variety of shape optimization problems with various constraints.

References

[AA13] C. J. S. Alves and P. R. S. Antunes. The method of fundamental solutions applied to some inverse eigenproblems. *SIAM J. Sci. Comput.*, 35(3):A1689–A1708, 2013.

[AF12] P. R. S. Antunes and P. Freitas. Numerical optimization of low eigenvalues of the Dirichlet and Neumann Laplacians. *J. Optim. Theory Appl.*, 154(1):235–257, 2012.

[AF16] P. R. S. Antunes and P. Freitas. Optimisation of eigenvalues of the Dirichlet Laplacian with a surface area restriction. *Appl. Math. Optim.*, 73(2):313–328, 2016.

[AG11] H. Anciaux and B. Guilfoyle. On the three-dimensional Blaschke-Lebesgue problem. *Proc. Amer. Math. Soc.*, 139(5):1831–1839, 2011.

[AH11] P. R. S. Antunes and A. Henrot. On the range of the first two Dirichlet and Neumann eigenvalues of the Laplacian. *Proc. R. Soc. Lond. Ser. A Math. Phys. Eng. Sci.*, 467(2130):1577–1603, 2011.

[Ant11] P. R. S. Antunes. Numerical calculation of eigensolutions of 3D shapes using the method of fundamental solutions. *Numer. Methods Partial Differential Equations*, 27(6):1525–1550, 2011.

[Ant16] P. R. S. Antunes. Maximal and minimal norm of Laplacian eigenfunctions in a given subdomain. *Inverse Problems*, 32(11):115003, 18, 2016.

[BB05] D. Bucur and G. Buttazzo. *Variational methods in shape optimization problems*. Progress in Nonlinear Differential Equations and their Applications, 65. Birkhäuser Boston, Inc., Boston, MA, 2005.

[BBF18] B. Bogosel, D. Bucur, and I. Fragalà. Phase field approach to optimal packing problems and related cheeger clusters. *Applied Mathematics & Optimization*, feb 2018.

[BH12] T. Bayen and D. Henrion. Semidefinite programming for optimizing convex bodies under width constraints. *Optim. Methods Softw.*, 27(6):1073–1099, 2012.

[BHL17] B. Bogosel, A. Henrot, and I. Lucardesi. Optimization of eigenvalues under constant width constraint. 2017.

[BLRO07] T. Bayen, T. Lachand-Robert, and E. Oudet. Analytic parametrization of three-dimensional bodies of constant width. *Arch. Ration. Mech. Anal.*, 186(2):225–249, 2007.

[BT05] T. Betcke and L. N. Trefethen. Reviving the method of particular solutions. *SIAM Rev.*, 47(3):469–491 (electronic), 2005.

[Buc12] D. Bucur. Minimization of the k-th eigenvalue of the Dirichlet Laplacian. *Arch. Ration. Mech. Anal.*, 206(3):1073–1083, 2012.

[BW18] S. Bartels and G. Wachsmuth. Numerical approximation of optimal convex shapes, 2018.

[CCP09] G. Carlier, M. Comte, and G. Peyré. Approximation of maximal Cheeger sets by projection. *M2AN Math. Model. Numer. Anal.*, 43(1):139–150, 2009.

[CFM09] V. Caselles, G. Facciolo, and E. Meinhardt. Anisotropic Cheeger sets and applications. *SIAM J. Imaging Sci.*, 2(4):1211–1254, 2009.

[DPV14] G. De Philippis and B. Velichkov. Existence and regularity of minimizers for some spectral functionals with perimeter constraint. *Appl. Math. Optim.*, 69(2):199–231, 2014.

[Gol60] M. Goldberg. Rotors in polygons and polyhedra. *Math. Comput*, 14:229–239, 1960.

[Gro96] H. Groemer. *Geometric applications of Fourier series and spherical harmonics*, volume 61 of *Encyclopedia of Mathematics and its Applications*. Cambridge University Press, Cambridge, 1996.

[Hen06] A. Henrot. *Extremum problems for eigenvalues of elliptic operators*. Frontiers in Mathematics. Birkhäuser Verlag, Basel, 2006.

[HO03] A. Henrot and E. Oudet. Minimizing the second eigenvalue of the Laplace operator with Dirichlet boundary conditions. *Arch. Ration. Mech. Anal.*, 169(1):73–87, 2003.

[HP18] A. Henrot and M. Pierre. *Shape variation and optimization*, volume 28 of *EMS Tracts in Mathematics*. European Mathematical Society (EMS), Zürich, 2018. A geometrical analysis, English version of the French publication [MR2512810] with additions and updates.

[Kar01] A. Karageorghis. The method of fundamental solutions for the calculation of the eigenvalues of the Helmholtz equation. *Appl. Math. Lett.*, 14(7):837–842, 2001.

[KLR06] B. Kawohl and T. Lachand-Robert. Characterization of Cheeger sets for convex subsets of the plane. *Pacific J. Math.*, 225(1):103–118, 2006.

[KW11] B. Kawohl and C. Weber. Meissner's mysterious bodies. *Math. Intelligencer*, 33(3):94–101, 2011.

[LN10] J. Lamboley and A. Novruzi. Polygons as optimal shapes with convexity constraint. *SIAM J. Control Optim.*, 48(5):3003–3025, 2009/10.

[LNP12] J. Lamboley, A. Novruzi, and M. Pierre. Regularity and singularities of optimal convex shapes in the plane. *Arch. Ration. Mech. Anal.*, 205(1):311–343, 2012.

[LRO05] T. Lachand-Robert and E. Oudet. Minimizing within convex bodies using a convex hull method. *SIAM J. Optim.*, 16(2):368–379, 2005.

[LRO07] T. Lachand-Robert and É. Oudet. Bodies of constant width in arbitrary dimension. *Math. Nachr.*, 280(7):740–750, 2007.

[Mei09] E. Meissner. Über die anwendung von fourier-reihen auf einige aufgaben der geometrie und kinematik. *Vierteljahrschrift der Naturforschenden Gesellschaft*, 54:309–329, 1909.

[MO14] Q. Mérigot and E. Oudet. Handling convexity-like constraints in variational problems. *SIAM J. Numer. Anal.*, 52(5):2466–2487, 2014.

[MP13] D. Mazzoleni and A. Pratelli. Existence of minimizers for spectral problems. *J. Math. Pures Appl. (9)*, 100(3):433–453, 2013.

[Mü09] M. Müller. Konvexe körper konstanter breite unter besonderer berücksichtigung des meissner-tetraeders. Diplomarbeit, Universität zu Köln, 2009.

[Ost10] B. Osting. Optimization of spectral functions of Dirichlet-Laplacian eigenvalues. *J. Comput. Phys.*, 229(22):8578–8590, 2010.

[Oud04] É. Oudet. Numerical minimization of eigenmodes of a membrane with respect to the domain. *ESAIM Control Optim. Calc. Var.*, 10(3):315–330 (electronic), 2004.

[Oud13] E. Oudet. Shape optimization under width constraint. *Discrete Comput. Geom.*, 49(2):411–428, 2013.

[Sch14] R. Schneider. *Convex bodies: the Brunn-Minkowski theory*, volume 151 of *Encyclopedia of Mathematics and its Applications*. Cambridge University Press, Cambridge, expanded edition, 2014.

[ŠGJ08] Z. Šír, J. Gravesen, and B. Jüttler. Curves and surfaces represented by polynomial support functions. *Theoret. Comput. Sci.*, 392(1-3):141–157, 2008.

[SW79] G. Salinetti and R. J.-B. Wets. On the convergence of sequences of convex sets in finite dimensions. *SIAM Rev.*, 21(1):18–33, 1979.

[Top06] V. A. Toponogov. *Differential geometry of curves and surfaces*. Birkhäuser Boston, Inc., Boston, MA, 2006. A concise guide, With the editorial assistance of Vladimir Y. Rovenski.

[Val64] F. A. Valentine. *Convex sets*. McGraw-Hill Series in Higher Mathematics. McGraw-Hill Book Co., New York-Toronto-London, 1964.